Ferromagnetism analysis of Mn-doped CuO thin films

Ferromagnetism analysis of Mn-doped CuO thin films

F Zhao[1]**, H M Qiu**[1]**, L Q Pan**[1]**, H Zhu**[2]**, Y P Zhang**[1,2]**, Z G Guo**[1]**, J H Yin**[1]**, X D Zhao**[1] **and John Q Xiao**[2]

[1] Department of Physics, University of Science and Technology Beijing, Beijing 100083, People's Republic of China
[2] Department of Physics and Astronomy, University of Delaware, Newark, DE 19706, USA

E-mail: lpan@sas.ustb.edu.cn

Abstract
Mn (6.6–29.8%)-doped CuO thin film fabricated on a thermally oxidized silicon substrate by radio-frequency magnetron sputtering has been reported. The films were structurally characterized using x-ray diffraction with Rietveld refinement. The analysis indicates that Mn uniformly substituted at the Cu position in the CuO lattice. 5% cation vacancies were detected at the Cu sites and are supposed to be responsible for the p-type electrical conduction of $Cu_{1-x}Mn_xO$ films. No evidence for large scale Mn aggregation was found in the composition range analyzed. The origin of ferromagnetism was analyzed in the context of competition among several interactions among Mn and Cu ions. A chain model was developed to simulate the ferromagnetic behavior with the random Mn distribution in the samples. The consistency between simulation and experiment strongly indicates that the ferromagnetism mainly arises from the super-exchange interactions of Mn–O–Cu–O–Mn coupling in the $[10\bar{1}]$ chain and Mn–O–Mn coupling contributes to the antiferromagnetism.

1. Introduction

Diluted magnetic semiconductors (DMSs) [1] have attracted considerable research effort for potential applications to spintronics and with the goal of identifying doped semiconducting materials with large magnetic moments and high Curie temperatures [2]. Since Dietl *et al* suggested that Mn-doped ZnO should show room-temperature ferromagnetism caused by exchange coupling between local spins and charge carriers as proposed by Zener [2, 3], extensive work has been done on transition-metal-doped oxide semiconductors [4–8], where room-temperature ferromagnetism has been observed. However, the origin of ferromagnetism in these materials is not well understood. Risbud *et al* proposed an antiferromagnetic coupling between nearest neighbors [9], while Norton *et al* suggested that the ferromagnetism could be caused by Co nanocrystallites embedded in ZnO when they investigated Co-doped ZnO [10]. What is the real mechanism responsible for the ferromagnetism? This question has not been completely resolved and an answer is still actively pursued.

Pure CuO is a compound associated with high-T_C superconductors [11] and crystallizes as a complicated monoclinic tenorite structure [12] exhibiting interesting antiferromagnetic ordering below 225 K [13]. The monoclinic unit cell contains four CuO molecules. In the (110) plane, each Cu atom is linked to four nearly coplanar O atoms at the corner of an almost rectangular parallelogram. The rather high Néel temperature indicates strong exchange interactions [13] and the matching of experimental and Heisenberg-model susceptibilities suggests that CuO could be classified as one-dimensional [14]. The exchange in the Cu–O–Cu chains along the $[10\bar{1}]$ direction are strongest and completely antiferromagnetic [15]. Although many different types of experiments have been carried out to determine various properties of the copper oxides, such as optical, transport, elastic, plastic, excitonic, spectroscopic and neutron scattering studies, little is known about the nature of ferromagnetism in DMSs on CuO. We reported the structural and magnetic properties of highly (111) oriented Mn-doped CuO films that have been fabricated on a thermally oxidized silicon substrate by radio-frequency magnetron sputtering in our previous work [16]. In the current paper, we have performed more detailed analysis on the crystallographic structure of the $Cu_{1-x}Mn_xO$ films using x-ray diffraction with Rietveld

Table 1. Refined structural data for $Cu_{1-x}Mn_xO$ films with $x = 15.2\%$ obtained using the GSAS program along with the reported structural data for CuO.

Sample	a (Å)	b (Å)	c (Å)	α (deg)	β (deg)	γ (deg)	V (Å^3)
CuO	4.653	3.410	5.108	90	99.48	90	79.94
$Cu_{1-x}Mn_xO$	4.707	3.334	5.078	90	100.02	90	78.48
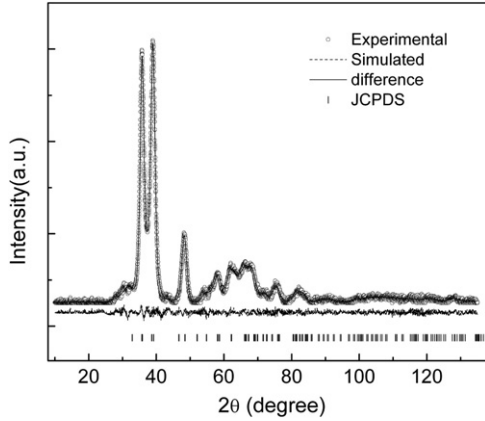
Figure 1. Observed (circle) and calculated (solid line) XRD profiles for the GSAS refinement of $Cu_{1-x}Mn_xO$ along with the plots of the difference between the observed and calculated profiles. The vertical bars indicate the position of the reflections on JCPDS.

refinement. A chain model is developed to simulate the ferromagnetic behavior of the samples and the results of theoretical calculations are reported to analyze the origin of ferromagnetism in Mn-doped CuO films.

2. Experimental result

Highly (111) oriented Mn (6.6%–29.8%)-doped CuO thin films have been fabricated on a thermally oxidized silicon substrate by radio-frequency magnetron sputtering. The x-ray photoelectron spectroscopy (XPS) result indicates that both the Cu and the Mn are in 2+ states [16]. To obtain more detailed information about the crystallographic structure of the films, we performed full pattern matching refinement of the x-ray diffraction spectra with the general structure analysis system (GSAS) program package. In the analysis, a space group of $C2/c$ was adopted. Instrumental broadening and zero shifting were obtained from the refinement of the x-ray spectrum of the Si powder. Figure 1 shows the x-ray spectrum with application of the refinement for the film doped with 15.2 at.% of Mn. Obviously, the fitted powder patterns are in agreement with the respective experimental XRD intensity data, noted by the R_p and R_{wp} factors, which present values of 3.6% and 4.8%. The refined lattice constants, a, b and c, are listed in table 1 along with the unit cell volume. The crystal structure remains almost unchanged in the Mn-doped CuO film except for a slight variation in the lattice constants. The lattice parameter a increases by 0.05, while b and c decrease by 0.08 and 0.03 Å, respectively. The lattice variation caused by the manganese insertion, indicated by the decrease in the unit cell volume from 79.9 to 78.5 Å^3, can be associated with the different sizes of a

Table 2. Ferromagnetic parameters of the samples.

Doping conc. (Mn%)	Curie temp. (K)	M_{CW} (μ_B/Mn), from CW	M_S (emu g^{-1})	M (μ_B/Mn)
6.6	0	4.4	NA	0
8.9	0	3.55	NA	0
15.2	86.4	3.1	5.31	0.47
17.7	93.8	2.48	6.60	0.51
26.6	98.5	2.28	10.41	0.54
29.8	99.5	2.34	11.24	0.52

manganese ion and a copper ion. Therefore, it is unlikely for Mn atoms to locate in the intermediate positions between Cu and O. If Mn takes the intermediate position, it will result in a large variation of lattice parameters due to Coulomb repulsion. Considering the high resistivity of the sample and the Rietveld refined result, we can conclude that Mn uniformly substitutes Cu in the CuO lattice. Analysis gives occupancies of 0.77 for Cu and 0.18 for Mn at the Cu site. It should be noted there are 5% vacancies at the copper sites. It is supposed that holes generated from Cu or Mn vacancies are responsible for p-type electrical conduction.

The ferromagnetism of the films was measured by a superconducting quantum interference device (SQUID, Quantum Design Co.) and the result is shown in table 2. Column 1 is the Mn doping concentration in the samples. The Curie temperatures given in column 2 were determined by magnetization versus temperature measurements. The magnetic susceptibility above T_C up to room temperature can be fitted well with the Curie–Weiss (CW) law and the magnetic moment per Mn ion obtained from CW fitting is given in column 3. We took the magnetizations at 5 T for sample saturation magnetizations as shown in column 4. The magnetic moment for each doped Mn atom in column 5 is defined to be the saturation magnetization over the total numbers of Mn ions in the samples. It can be seen that obviously the Mn average moment is around 0.5 μ_B with no correspondence to the doping concentration. The dependence of the magnetic susceptibility upon temperature for 17.7% Mn-doped CuO under 1000 Oe magnetic field is shown in figure 2. The inset of figure 2 shows the linear dependence of the magnetic susceptibility at 5 K on different Mn doping concentrations.

3. Model analysis

Filippetti and Fiorentini [15] investigated the interplay of bonding and magnetism in CuO by a first-principles self-interaction free-density approach and revealed the main interaction connects Cu atoms as Cu–O–Cu segments with angles of 145°, and the second main interaction has a
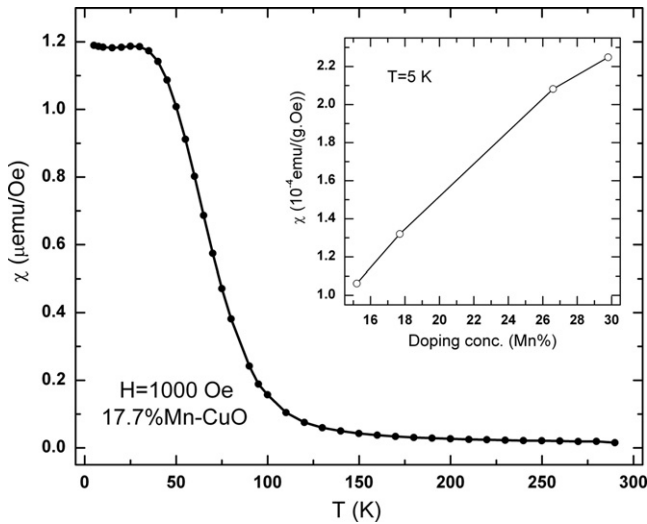
Figure 2. Magnetic susceptibility as a function of the temperature for 17.7% Mn-doped CuO under 1000 Oe magnetic field. The inset is the magnetic susceptibility at 5 K for different Mn dopings.

magnitude less than half the magnitude of the main interaction. As an approximation, we propose a simple 'chain model' to explain the ferromagnetism and assume that magnetic coupling in this system is only in the [10$\bar{1}$] direction.

The Rietveld refinement confirms that Mn randomly substitutes Cu in the CuO lattice. Although the spin order can be destroyed by doping Mn, most Cu maintains its original spin order at low temperature. A super-exchange interaction between Mn^{2+} and Cu^{2+} exists through O^{2-}, which induces the spins of the two nearest Mn ions in the Mn–O–Mn configuration to be antiparallel and those of the two second-nearest Mn ions in the Mn–O–Cu–O–Mn configuration to be parallel. Very high resistivities suggest the carrier densities of $Cu_{1-x}Mn_xO$ are too low to provide sufficient mediation [17] to align the spins of neighboring Mn ions at low temperature. Furthermore, we deposited thin films in an atmosphere lacking O_2 with the same Mn concentration, and the films showed the same magnetic behavior. Therefore, the carrier mediate mechanism is not applicable to this case. On the other hand, an exchange between Mn spins and carriers or Coulomb interaction between Mn ions and carriers can also be excluded [16]. Therefore, we suppose the ferromagnetism arises from the ferromagnetic coupling between Mn ions mediated by Cu ions. We then develop a 'chain model' to simulate the ferromagnetic behavior in Mn-doped CuO.

The possible coupling forms in the [10$\bar{1}$] direction in Mn-doped CuO films are shown in figure 3. The Mn ion

in a Cu–O–Cu–O–Mn–O–Cu–O–Cu segment easily switches its spin ordering and the exchange with other Mn ions is weak. We believe this represents paramagnetic coupling or a spin glass. The super-exchange interaction between nearest-neighboring Mn ions through O^{2-} in Mn–O–Mn segments leads to antiferromagnetic coupling, and a super-exchange interaction between nearest-neighboring Mn and Cu ions in Mn–O–Cu–O–Mn segments leads to ferromagnetic coupling. In this chain model, Mn ions with a +2 valence randomly substitute Cu ions in the CuO lattice. The magnetic moment of Cu is 0.68 μ_B [13], while the theoretical moment of Mn^{2+} is 5.92 μ_B, which cannot be completely owing to the inter-coupling intensity between the two transition metals. Moreover, the magnetic moment will be folded because of the angle between the O–Mn–O coupling direction and the [10$\bar{1}$] direction. We estimated the Mn^{2+} moment is about 5.92 μ_B in a paramagnetic state and 2.5 μ_B in a ferromagnetic state for the following calculation.

4. Discussion and conclusion

Based on the above chain model and supposing that Mn ions randomly substitute Cu ions in the CuO lattice, we calculated the average moment of Mn and the saturation magnetization of the samples at $T < T_C$ in the ferromagnetic state by simply summing up all of the magnetization of ferromagnetic coupling in a virtual Mn-doped CuO crystal. To prove the reliability of our calculations, we compared the calculated results with the experimental data as shown in figures 4 and 5. The conclusions drawn from figures 4 and 5 are as follows.

For a simulation at a low Mn concentration (0–10%), the possibility of a Cu ion neighboring with two Mn ions in Mn–O–Cu–O–Mn ferromagnetic coupling is very low, but the possibility of an isolated Mn ion neighboring with two Cu ions in Cu–O–Cu–O–Mn–O–Cu–O–Cu quasi-paramagnetic coupling is very high. Therefore, the calculated saturation magnetization is low, the average magnetic moment of Mn is even negligible, and in this range paramagnetism prevails. For the real samples with Mn concentrations of 6.6% and 8.9%, the distances between ferromagnetic Mn atoms seem too great to keep the same alignment of Mn spins, especially for such a low carrier density, so no ferromagnetic behavior was observed whereas paramagnetic behavior was. As the Mn concentration rises to about 10–20%, the percentage of Mn ions undergoing ferromagnetic coupling grows more quickly than the percentage undergoing Mn–O–Mn antiferromagnetic coupling, while the percentage
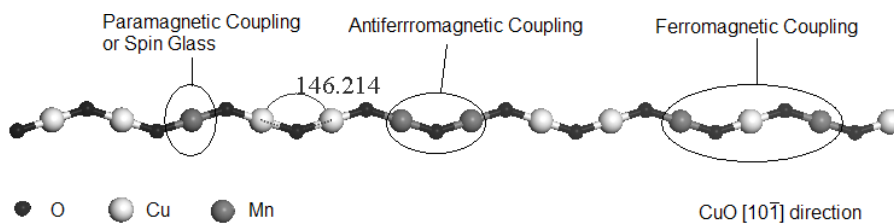

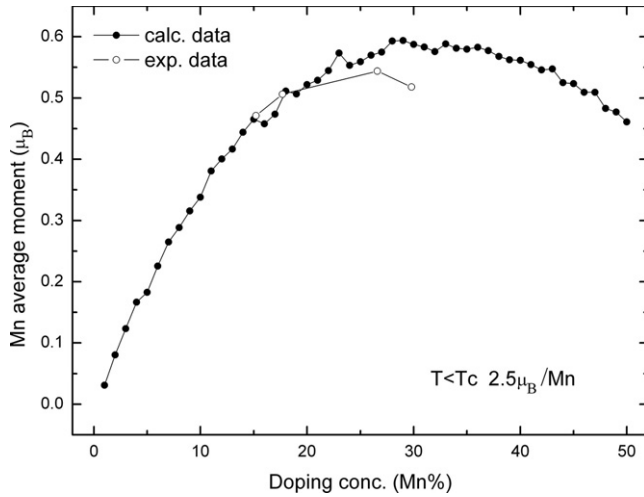**Figure 3.** Possible coupling ways on the CuO [10$\bar{1}$] direction.

Figure 4. Mn average moment as a function of different concentrations in Mn doped-CuO.
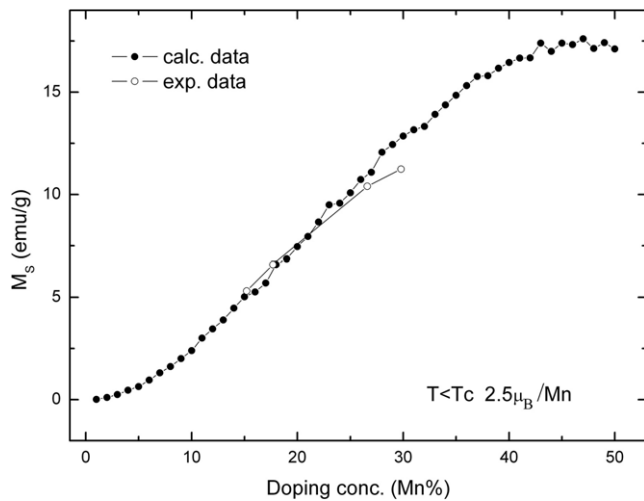

Figure 5. Saturation magnetization M_S as a function of different concentrations in Mn-doped CuO.

Figure 6. Paramagnetic moment as a function of different concentrations of Mn-doped CuO.

of Mn ions undergoing quasi-paramagnetic coupling decreases from 65% to 41%. Therefore, the simulated saturation magnetization increases remarkably and the simulated average magnetic moment of Mn becomes noticeable, which agrees well with the experimental data. When the Mn concentration is relatively high ($>20\%$), the percentage of Mn atoms undergoing antiferromagnetic coupling quickly increases while the percentage of ions undergoing ferromagnetic coupling nearly becomes a maximum and the percentage of ions undergoing paramagnetic coupling becomes a minimum. In this range, the rise of calculated saturation magnetization versus Mn percentage is mainly attributable to the higher Mn concentration because the calculated average magnetic moment of Mn is nearly constant close to its maximum value. Although the simulated magnetization is higher than that from the experiment for a high doping concentration, it is clear that the simulated and experimental data have a similar tendency. In fact, the magnetization of the samples has not reached saturation when the magnetic field is 5 T at
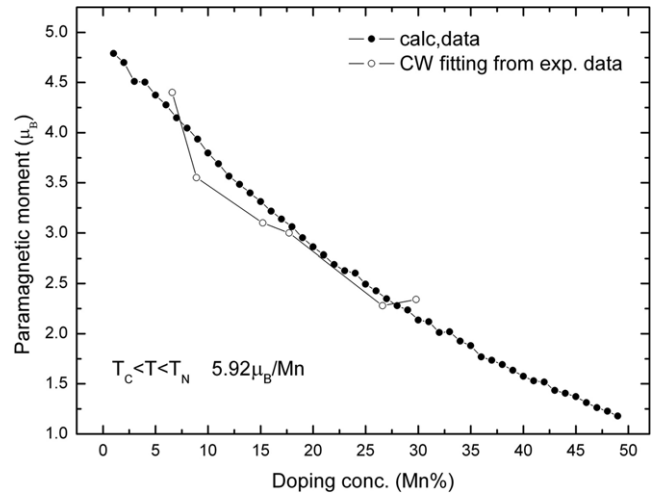
5 K. Therefore, the saturation magnetization and Mn average magnetic moment in real systems should be larger because we took the magnetizations at 5 T for sample saturation magnetizations.

To evaluate the rationality of our model, we performed a paramagnetic simulation in which we assumed that ferromagnetic coupling has become paramagnetic coupling for temperatures higher than T_c while Mn–O–Mn and Cu–O–Cu antiferromagnetic coupling still occurs due to their strong super-exchange interactions ($T < T_N$). Here, we assume the Mn^{2+} magnetic moment is equal to the theoretical value of 5.0 μ_B, all Cu^{2+} ions maintain their antiferromagnetic alignment and all neighboring Mn ions are employed in antiferromagnetic coupling without any contribution to paramagnetism. So we calculated the Mn average paramagnetic moment by adding all the paramagnetic couplings and then divided by the amount of Mn atoms. The simulation result is given in figure 6 and has similar tendencies to that of the CW fitting ($T > T_c$) result. The simulation suggests the increasing Mn concentration leads to more antiferromagnetic coupling that directly reduces the paramagnetic moment.

The likely reason for the differences between simulation and experimental data is the spatial non-uniformity of the Mn distribution in small regions. If Mn–O–Mn coupling has a lower energy than Mn–O–Cu coupling, the Mn atoms will prefer Mn–O–Mn coupling in a small region, especially when the substrate temperature is high. If this happens, more antiferromagnetic coupling will appear than we predict. This will lead to lower saturation magnetization, a lower Mn average magnetic moment and a lower paramagnetic moment than in the simulation results. In addition, the apex of the Mn average magnetic moment curve will be further to the low Mn percentage side than for the simulation. Another possible explanation is, as we have found in x-ray refraction, when the Mn dopant concentration increases, the structure varies toward amorphism-like. That will make our chain model develop from reasonable to faint to interpret the experimental results because of the structural deterioration. Mn–Mn coupling from

the non-$[10\bar{1}]$ direction will change the Cu–Mn and Mn–Mn bond angles and reduce the stiffness of coupling in the $[10\bar{1}]$ direction, and finally decrease the embodying moment of the Mn atom and increase the Mn average paramagnetic moment.

The consistency of simulation with experimental data strongly indicates that the exchanges of Mn–O–Cu–O–Mn ferromagnetic coupling and Mn–O–Mn antiferromagnetic coupling in the $[10\bar{1}]$ chain dominate the magnetic properties of the samples. It is reasonable that we suppose Mn atoms equally substitute Cu atoms in the CuO lattice for the present samples. If Mn atoms aggregate on a large scale and eventually form clusters, the experimental points and tendencies will largely deviate from the simulation.

In summary, a highly (111)-oriented Mn-doped CuO thin film has been fabricated. The Rietveld refinement analysis confirms that Mn has uniformly substituted Cu positions in the CuO lattice. 5% vacancies are detected at Cu sites and are supposed to be responsible for the p-type electrical conduction of Mn-doped CuO films. A chain model has been developed to simulate the ferromagnetic behavior with a random Mn distribution in the samples. The consistency of the simulation and experiment strongly indicates two conclusions: (1) no large scale Mn aggregation forms and (2) the exchanges of Mn–O–Cu–O–Mn and Mn–O–Mn–O–Mn coupling in the $[10\bar{1}]$ chain stabilize the ferromagnetism of samples.

Acknowledgments

References

[1] Furdyna J K 1988 *J. Appl. Phys.* **64** R29
[2] Dietl T, Ohno H, Matsukura F, Cibert J and Ferraud D 2000 *Science* **287** 1019
[3] Zener C 1951 *Phys. Rev.* **81** 440
[4] Fukumura T, Jin Z W, Kawasaki M, Shono T, Hasegawa T, Koshihara S and Koinuma H 2001 *Appl. Phys. Lett.* **78** 958
[5] Ogale S B *et al* 2003 *Phys. Rev. Lett.* **91** 077205
[6] Matsumoto Y 2001 *Science* **294** 1003
[7] Hong N Y H, Sakai J and Hassini A 2004 *Appl. Phys. Lett.* **84** 2602
[8] Janisch R, Gopal P and Spaldin N A 2005 *J. Phys.: Condens. Matter* **17** R657
[9] Risbud A S, Spaldin N A, Chen Z Q, Stemmer S and Seshadri R 2003 *Phys. Rev.* B **68** 205202
[10] Norton D P, Overberg M E, Pearton S J, Pruessner K, Budai J D, Boatner L A, Chisholm M F, Lee J S, Khim Z G, Park Y D and Wilson R G 2003 *Appl. Phys. Lett.* **83** 5488
[11] Sohma M, Kawaguchi K and Fujii Y 1995 *J. Appl. Phys.* **77** 1189
[12] Asbrink S and Norrby L J 1970 *Acta Crystallogr.* B **26** 8
[13] Yang B X, Tranquada J M and Shirane G 1988 *Phys. Rev.* B **38** 174
[14] Shimizu T, Matsumoto T, Goto A, Chandrasekhar Rao T V, Yoshimura K and Kosuge K 2003 *Phys. Rev.* B **68** 224433
[15] Filippetti A and Fiorentini V 2005 *Phys. Rev. Lett.* **95** 086405
[16] Zhu H, Zhao F, Pan L, Zhang Y, Fan C and Xiao J Q 2007 *J. Appl. Phys.* **101** 09H111
[17] Griffin K A, Pakhomov A B, Wang C M, Heald S M and Krishnan K M 2005 *Phys. Rev. Lett.* **94** 157204